The Plant Cell, Vol. 32: 226–241, January 2020, www.plantcell.org © 2020 ASPB.

AP2/ERF Transcription Factors Integrate Age and Wound Signals for Root Regeneration[OPEN]

Bin-Bin Ye,[a,b] Guan-Dong Shang,[a,b] Yu Pan,[c] Zhou-Geng Xu,[a,b] Chuan-Miao Zhou,[a] Ying-Bo Mao,[d] Ning Bao,[e] Lijun Sun,[c] Tongda Xu,[f] and Jia-Wei Wang[a,g,1]

[a] National Key Laboratory of Plant Molecular Genetics, Chinese Academy of Sciences Center for Excellence in Molecular Plant Sciences, Institute of Plant Physiology and Ecology, 200032 Shanghai, P. R. China
[b] University of Chinese Academy of Sciences, 200032 Shanghai, P. R. China
[c] School of Life Sciences, Nantong University, Nantong, 226019 Jiangsu, P. R. China
[d] Chinese Academy of Sciences Key Laboratory of Insect Developmental and Evolutionary Biology, Chinese Academy of Sciences Center for Excellence in Molecular Plant Sciences, Institute of Plant Physiology and Ecology, 200032 Shanghai, P. R. China
[e] School of Public Health, Nantong University, Nantong, 226019 Jiangsu, P. R. China
[f] Fujian Agriculture and Forestry University-University of California Riverside Joint Center, Horticulture Biology and Metabolomics Center, Haixia Institute of Science and Technology, Fujian Agriculture and Forestry University, 350002 Fuzhou, P. R. China
[g] ShanghaiTech University, Shanghai 200031, P. R. China

ORCID IDs: 0000-0001-9171-3433 (B.-B.Y.); 0000-0002-9509-0314 (G.-D.S.); 0000-0003-4219-3448 (Y.P.); 0000-0001-7682-3482 (Z.-G.X.); 0000-0001-5602-0930 (C.-M.Z.); 0000-0003-4599-3619 (Y.-B.M.); 0000-0002-5630-4359 (N.B.); 0000-0003-4022-8803 (L.S.); 0000-0003-3398-9217 (T.X.); 0000-0003-3885-6296 (J.-W.W.).

Age and wounding are two major determinants for regeneration. In plants, the root regeneration is triggered by wound-induced auxin biosynthesis. As plants age, the root regenerative capacity gradually decreases. How wounding leads to the auxin burst and how age and wound signals collaboratively regulate root regenerative capacity are poorly understood. Here, we show that the increased levels of three closely-related miR156-targeted Arabidopsis (*Arabidopsis thaliana*) SQUAMOSA PROMOTER BINDING PROTEIN-LIKE (SPL) transcription factors, SPL2, SPL10, and SPL11, suppress root regeneration with age by inhibiting wound-induced auxin biosynthesis. Mechanistically, we find that a subset of APETALA2/ETHYLENE RESPONSE FACTOR (AP2/ERF) transcription factors including ABSCISIC ACID REPRESSOR1 and ERF109 is rapidly induced by wounding and serves as a proxy for wound signal to induce auxin biosynthesis. In older plants, SPL2/10/11 directly bind to the promoters of *AP2/ERFs* and attenuates their induction, thereby dampening auxin accumulation at the wound. Our results thus identify AP2/ERFs as a hub for integration of age and wound signal for root regeneration.

INTRODUCTION

Among the universal changes that occur with age in multicellular organisms is the decline in regenerative capacity. In mammals, for example, the heart quickly loses its capacity to regenerate within a brief period after birth (Porrello et al., 2011). Remyelination, the phenomenon by which new myelin sheaths are generated around axons in the adult central nervous system, declines with increasing age (Ruckh et al., 2012). The factors that are likely involved include accumulated DNA mutations, reduced number of stem cells, decreased cell proliferative capacity, and disturbed metabolic function (Wells and Watt, 2018). In plants, the regenerative capacity also progressively decreases with age. For example, the number of newly formed sprouts decreased significantly in *Calluna vulgari* plants that were more than 6 years old (Berdowski and Siepel, 1998). Similarly, the shoot regenerative capacity declines as *Quercus euboica* ages (Kartsonas and Papafotiou, 2007).

Plant hormones play pivotal roles in regeneration (Birnbaum and Sánchez Alvarado, 2008; Sena and Birnbaum, 2010; Perianez-Rodriguez et al., 2014; Pulianmackal et al., 2014; Su and Zhang, 2014; Xu and Huang, 2014; Ikeuchi et al., 2016; Kareem et al., 2016; Sang et al., 2018). It is well known that cytokinin induces shoot regeneration whereas auxin promotes root regeneration (Skoog and Miller, 1957). There are different ways to regenerate roots. In the tissue culture experiments, high auxin/cytokinin in root induction medium triggers the reprogramming of callus, a group of dedifferentiated cells initiated from xylem-pole pericycle cells of root explants and pericycle-like cells of aerial organs, into roots (Atta et al., 2009; Sugimoto et al., 2010; Ikeuchi et al., 2016). By contrast, root tip regeneration follows the developmental stages of embryonic patterning and is guided by spatial information provided by complementary hormone domains (Efroni et al., 2016). The detached Arabidopsis (*Arabidopsis thaliana*) leaf or hypocotyl can also regenerate roots on hormone-free B5 medium (Liu et al., 2014). It is proposed that the regeneration-competent cells in the pericycle around the wound undergo four sequential steps to initiate adventitious roots (Xu, 2018).

The molecular mechanism by which shoot regenerative capacity is affected by age during tissue culture has been well documented. Our previous work reveals an important role of

[1] Address correspondence to jwwang@sippe.ac.cn.
The author(s) responsible for distribution of materials integral to the findings presented in this article in accordance with the policy described in the Instructions for Authors (www.plantcell.org) is: Jia-Wei Wang (jwwang@sippe.ac.cn).
[OPEN]Articles can be viewed without a subscription.
www.plantcell.org/cgi/doi/10.1105/tpc.19.00378

microRNA156 (miR156), the master regulator of juvenility, in shoot regeneration (Poethig, 2009; Yu et al., 2015c). miR156 targets a group of transcription factors named SQUAMOSA PROMOTER BINDING PROTEIN-LIKE (SPL; Rhoades et al., 2002; Schwab et al., 2005; Wu and Poethig, 2006; Gandikota et al., 2007). Juvenile plants exhibit a high cytokinin response and regenerative capacity. As a plant ages, miR156 levels decline, alleviating the repression of its SPL targets (Wang et al., 2009; Yamaguchi et al., 2009; Xu et al., 2018). SPL directly inhibits the transcriptional activity of B-type ARABIDOPSIS RESPONSE REGULATORs and thereby impairs shoot regenerative capacity (Zhang et al., 2015). miR156 is also involved in de novo root regeneration in Arabidopsis (Xu et al., 2016; Ye et al., 2019). The hypocotyls from the plants with low miR156 activity produce fewer adventitious roots than those from wild type. Notably, this phenomenon seems to be evolutionarily conserved. The same positive relationship between miR156 level and rooting capacity has been found in *Malus xiaojinensis* and *Medicago sativa* (Aung et al., 2017; Xu et al., 2017). However, the molecular mechanism by which miR156/SPL regulates root regenerative capacity is poorly understood.

Here, we find that miR156-targeted SPLs have divergent roles in plant regeneration. Whereas the SPL9 subfamily suppressed shoot regeneration, the SPL10 subfamily specifically suppressed root regeneration by inhibiting auxin burst in response to wounding. By the combination of RNA-sequencing (RNA-seq) and chromatin immunoprecipitation followed by sequencing (ChIP-seq), we further identified a subset of APETALA2/ETHYLENE RESPONSE FACTOR (AP2/ERF) transcription factors as the proxy for wound signal to induce auxin biosynthesis, and these transcription factors act as a hub for integration of age and wound signal.

RESULTS

Divergent Roles of miR156-Targeted SPLs in Plant Regeneration

In Arabidopsis, miR156 targets 11 *SPL* genes (Xing et al., 2013). Whether all the SPL members contribute to root regeneration is still unknown. To address this question, we examined root regeneration capacity by culturing leaf explants on B5 medium without added exogenous hormones under long-day conditions (Liu et al., 2014). To avoid the impact of leaf age on regenerative capacity, the first/second (early/juvenile), third/fourth (mid), and sixth (late/adult) Arabidopsis leaves of the same developmental stage (3 mm in length) were used. Consistent with published results (Xu et al., 2016), the rooting capacity was progressively decreased with plant age in wild type (Supplemental Figures 1A and 1B). The first to second leaf explants exhibited higher miR156 level than the sixth leaf explants (Supplemental Figure 1C).

Blocking the function of miR156 by overexpression of *MIM156* (mimicry of miR156) greatly reduced adventitious root formation (Supplemental Figures 1D and 1E). An opposite trend was observed when miR156 was overexpressed by constitutive *35S* promoter (Supplemental Figures 1D and 1E). Notably, the same relationship between miR156 level and rooting capacity was found in poplar tree (*Populus*; Supplemental Figures 1F and 1G), indicating that the role of miR156 in rooting is evolutionarily conserved (Wang et al., 2011).

We next performed the regeneration experiments using the first to second, third to fourth, and sixth leaf explant of *spl* single and high-order mutants. *SPL9* and *SPL15* have been reported to play an important role in shoot regeneration (Zhang et al., 2015). The sixth leaf explants of *spl9 spl15* exhibited the same rooting rate as wild type (Figures 1A and 1B). *SPL2*, *SPL10*, and *SPL11* constitute another miR156-targeted *SPL* subfamily. Because *SPL10* and *SPL11* are located in the same genetic locus, we generated *spl10 spl11* double mutants by the clustered regularly interspaced short palindromic repeats (CRISPR)/Cas9 technology (Supplemental Figures 2A to 2C; Ran et al., 2017; Yin et al., 2017). Compared to wild type, *spl10 spl11* showed increased rooting capacity (Figures 1A to 1C; Supplemental Figures 2D to 2I). This phenotype was further enhanced in *spl2 spl10 spl11* triple mutants (Figures 1A to 1C; Supplemental Figures 2D to 2I). Intriguingly, both *spl10 spl11* and *spl2 spl10 spl11* triple mutant did not affect shoot regeneration capacity in tissue culture (Supplemental Figure 2J and 2K).

We then generated *SPL9*- and *SPL10*-inducible lines (*pSPL9:rSPL9-GR* and *pSPL10:rSPL10-GR*), in which miR156-resistant forms of *SPLs* (*rSPL*) were fused to the hormone binding domain of rat glucocorticoid receptor (GR) and expressed from their own promoters. Treatment with the steroid hormone ligand dexamethasone (DEX), which leads to a translocation of the rSPL9/10-GR fusion protein from the cytoplasm to the nucleus, resulted in the same phenotype as the transgenic plants expressing *rSPL9/10* (*pSPL9:rSPL9/pSPL10:rSPL10*; Supplemental Figure 3A). In the absence of DEX, *pSPL9:rSPL9-GR* and *pSPL10:rSPL10-GR* rooted as wild type (Figure 1D; Supplemental Figure 4A). By contrast, after application of DEX, the rooting capacity of *pSPL10:rSPL10-GR* was nearly abolished, whereas that of *pSPL9:rSPL9-GR* remained unchanged (Figure 1D; Supplemental Figure 4A).

To probe the reason why *SPL10/11*, but not *SPL9/15*, represses root regeneration, we performed a promoter swapping experiment by generating *pSPL10:rSPL9*, *pSPL9:rSPL10*, *pSPL10:rSPL9-GR*, and *pSPL9:rSPL10-GR*. Both *pSPL10:rSPL9* and *pSPL9:rSPL10* accelerated the juvenile-to-adult phase transition (Supplemental Figure 3B). Intriguingly, *pSPL10:rSPL9* exhibited the same low rooting rate as *pSPL10:rSPL10* plants (Figure 1F; Supplemental Figure 4C). Consistently, *pSPL9:rSPL10* did not show altered rooting rate in comparison to wild type (Figure 1F; Supplemental Figure 4C). Similar results were obtained using *pSPL10:rSPL9-GR* and *pSPL9:rSPL10-GR* as explants (Figure 1E; Supplemental Figure 4B).

Analyses of *SPL9* and *SPL10* promoter β-Glucuronidase (GUS) reporter lines (two independent lines) revealed that *pSPL10:GUS* showed stronger staining in the procambium cells and some xylem parenchyma cells than *pSPL9:GUS* (Figures 1G to 1J; Supplemental Figures 3C to 3F), suggesting that the difference in promoter strength may underlie the functional divergence in root regeneration between SPL9/15 and SPL10/11. Consistent with the notion that *SPL10* and *SPL11* play redundant roles in rooting, *SPL11* exhibited the same expression pattern as *SPL10* (Supplemental Figure 3G). Taking these observations together, we conclude that the SPL9 subfamily is important for shoot

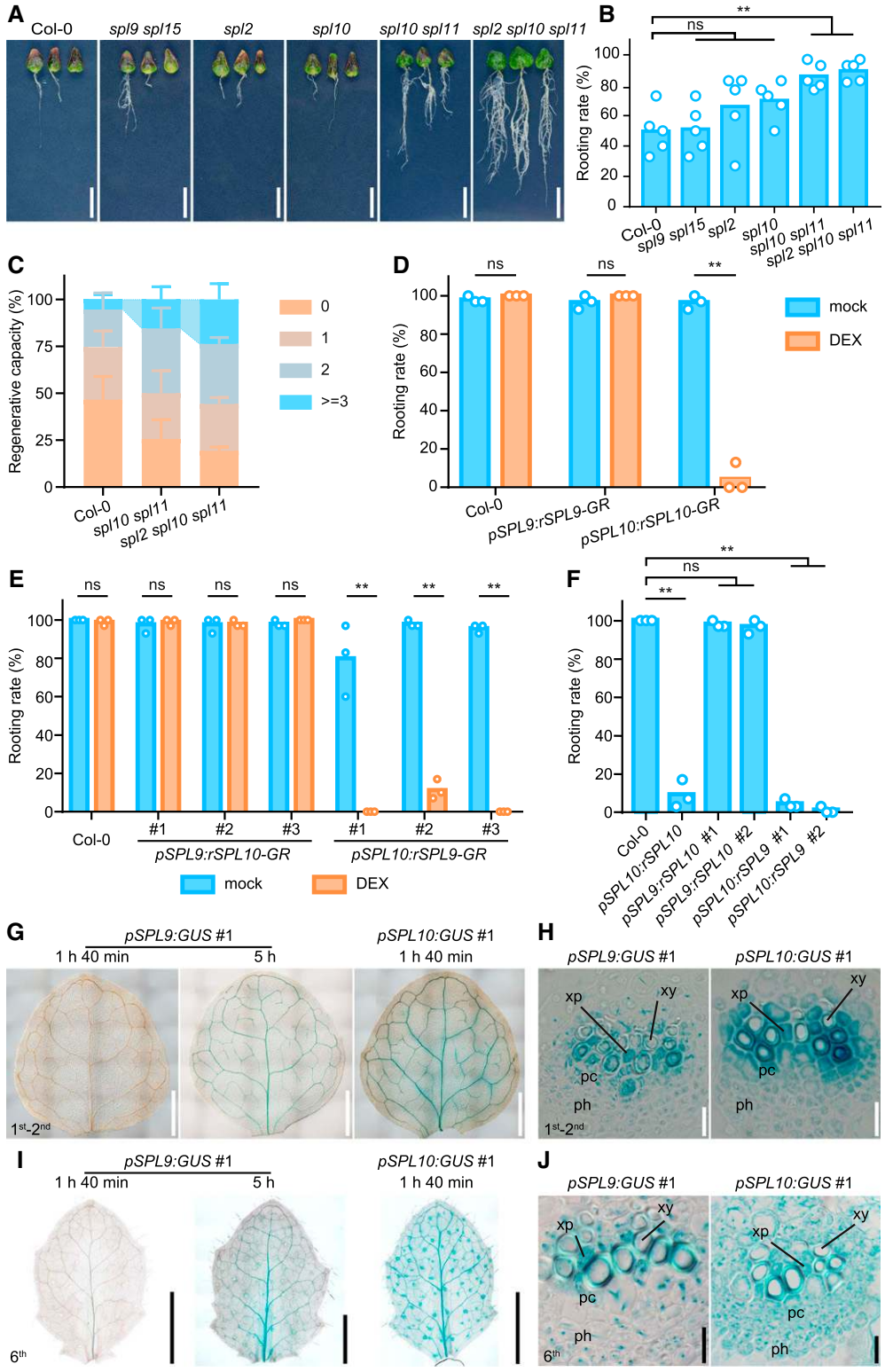

Figure 1. SPL10 Subfamily Regulates Rooting.

(A) Root regeneration assays using the sixth leaf explants from wild type and *spl* mutants. Pictures were taken at 20 DAC on B5 media. Scale bar = 1 cm.

regeneration, whereas SPL2, SPL10, and SPL11 play a dominant role in root regeneration.

SPL2/10/11 Regulate Root Regenerative Capacity Partially through Auxin

The formation of adventitious roots is triggered by the accumulation of auxin at the wound after leaf detachment (Xu, 2018). The impairment of root regeneration in adult wild type and *p35S*:*MIM156* and *pSPL10*:*rSPL10* plants, therefore, might be caused by defects in auxin biosynthesis or signal transduction. To distinguish between these two possibilities, we first examined the auxin responsiveness using DR5 as a reporter (Sabatini et al., 1999). Consistent with published results, the *DR5* expression was low before wounding (Liu et al., 2014; Chen et al., 2016b). After 1 d of leaf detachment, strong DR5 signals were observed in mesophyll cells and the vasculature near the wound in the first to second leaf (Figure 2A). By contrast, *DR5* expression was not greatly increased in both wound sites of the third to fourth and fifth to sixth leaves (Figure 2A; Supplemental Figure 5A). Comparison of the first to second leaves among wild type, *p35S*:*MIR156*, and *p35S*:*MIM156* further confirmed a positive relationship between miR156 level and the enhancement of *DR5* expression during root regeneration (Figures 2B and 2C; Supplemental Figures 5B and 5C).

To validate our results, we measured free indole-3-acetic acid (IAA) levels in wild type, *spl2 spl10 spl1*, and *pSPL10*:*rSPL10* explants. An auxin burst was evident in the first to second wild-type leaves at 2 d after culturing (DAC; Figure 2D). This effect was greatly suppressed in the fifth to sixth leaves (Figure 2D). In agreement with this, the accumulation of IAA was attenuated in the first to second leaves of *pSPL10*:*rSPL10* (Figure 2E) but boosted in the sixth leaf of *spl2 spl10 spl11* mutant (Figure 2F; Supplemental Figure 5D).

We next examined the expression of genes involved in auxin biosynthesis. *WEAK ETHYLENE INSENSITIVE2/ANTHRANILATE SYNTHASE alpha1* and *WEI7/ANTHRANILATE SYNTHASE beta1* (*ASB1*) genes that encode alpha- and beta-subunits of a rate-limiting enzyme in Trp biosynthesis pathway have a major role in Trp-dependent auxin biosynthesis (Stepanova et al., 2005, 2008; Tao et al., 2008). *TRYPTOPHAN AMINOTRANSFERASE OF ARABIDOPSIS1* (*TAA1*) catalyzes the conversion of Trp to indole-3-pyruvate (Stepanova et al., 2008). Compared to wild type, the expression of the *ASA1*, *ASB1*, and *TAA1* was low in *pSPL10*:*rSPL10* (Figure 2G; Supplemental Figure 5E). Upon leaf detachment, both *ASA1* and *ASB1* were induced in the first to second wild-type leaves within 2 d, whereas *TAA1* level remained constant. The upregulation of *ASA1* and *ASB1* was significantly suppressed in *pSPL10*:*rSPL10* (Figure 2G; Supplemental Figure 5E). When the sixth leaves were used as explants, the induction of *ASA1* was compromised in wild type but still evident in *spl2 spl10 spl11* mutant (Figure 2H). Thus, these results support the notion that the reduced rooting capacity of *pSPL10*:*rSPL10* is likely caused by a reduced amount of auxin in leaf explants.

We then asked whether exogenous auxin is sufficient to rescue the rooting defects of *pSPL10*:*rSPL10* plants. Compared to mock, the addition of IAA led to increased rooting rate of the first to second leaves of *pSPL10*:*rSPL10* in a dose-dependent manner (Figure 2I; Supplemental Figure 5F). This effect was also observed in the sixth wild-type leaves but to a lesser extent in *spl2 spl10 spl11* mutant background (Figure 2J; Supplemental Figure 5G). It should be noted that IAA could not fully rescue the rooting defects of *pSPL10*:*rSPL10*, implying that SPL10 does not suppress root regeneration exclusively through modulating auxin biosynthesis.

Identification of Direct Targets of SPL10 during Root Regeneration

The mechanism by which auxin sequentially induces root founder cell specification and cell fate transition has been well studied (Xu, 2018). However, the primary wounding response within hours during root regeneration is largely unknown. We harvested wild-type and *pSPL10*:*rSPL10* leaf explants at 0 and 4 h after leaf detachment. Total RNAs were extracted and subjected to RNA-seq analyses. In wild type, a total of 3,221 genes were differentially

Figure 1. (continued).

(B) Quantitative analysis of root regenerative rate of the sixth leaf explants in *spl* single and high-order mutants at 20 DAC. The rooting rate was represented by the percentage of leaf explants with regenerated roots. Data are from five independent experiments. Bars show mean. One-way ANOVA was performed followed by a Tukey's multiple comparisons test. $^{**}P < 0.01$; ns, not significant.

(C) The root regenerative capacity of the sixth leaf explants from wild type, *spl10 spl11*, and *spl2 spl10 spl11* at 12 DAC. The regenerative capacity was represented by the percentage of leaf explants with different number of regenerated roots. Data are from three independent experiments. Bars show mean ± SD.

(D) The rooting rate of leaf explants cultured on B5 medium without (mock) or with 10 μM of DEX treatment at 20 DAC. Data are from three independent experiments. Bars show mean. Two-sided Student's *t* test was performed. $^{**}P < 0.01$; ns, not significant.

(E) The rooting rate of leaf explants cultured on B5 medium without (mock) or with 10 μM of DEX treatment at 20 DAC. Data are from three independent experiments. Bars show mean. Two-sided Student's *t* test was performed. $^{**}P < 0.01$; ns, not significant.

(F) The rooting rate of leaf explants overexpressing *rSPL9* or *rSPL10* at 20 DAC. Data are from three independent experiments. Bars show mean. One-way ANOVA was performed followed by a Tukey's multiple comparisons test. $^{**}P < 0.01$; ns, not significant.

(G) and **(I)** Expression pattern of *SPL9* and *SPL10* promoter GUS reporters. The first to second leaves **(G)** and the sixth leaves **(I)** were stained for 5 h for *pSPL9*:*GUS* and 1 h 40 min for *pSPL10*:*GUS*. Scale bar = 1 mm. Three independent experiments were performed ($n = 15$ for each experiment). One representative picture is shown.

(H) and **(J)** Transverse section of *pSPL9*:*GUS* and *pSPL10*:*GUS* reporters. The first to second leaves **(H)** and the sixth leaves **(J)** were stained for the same time (24 h). xy, xylem; xp, xylem parenchyma cell; pc, procambium; ph, phloem. Scale bar = 10 μm.

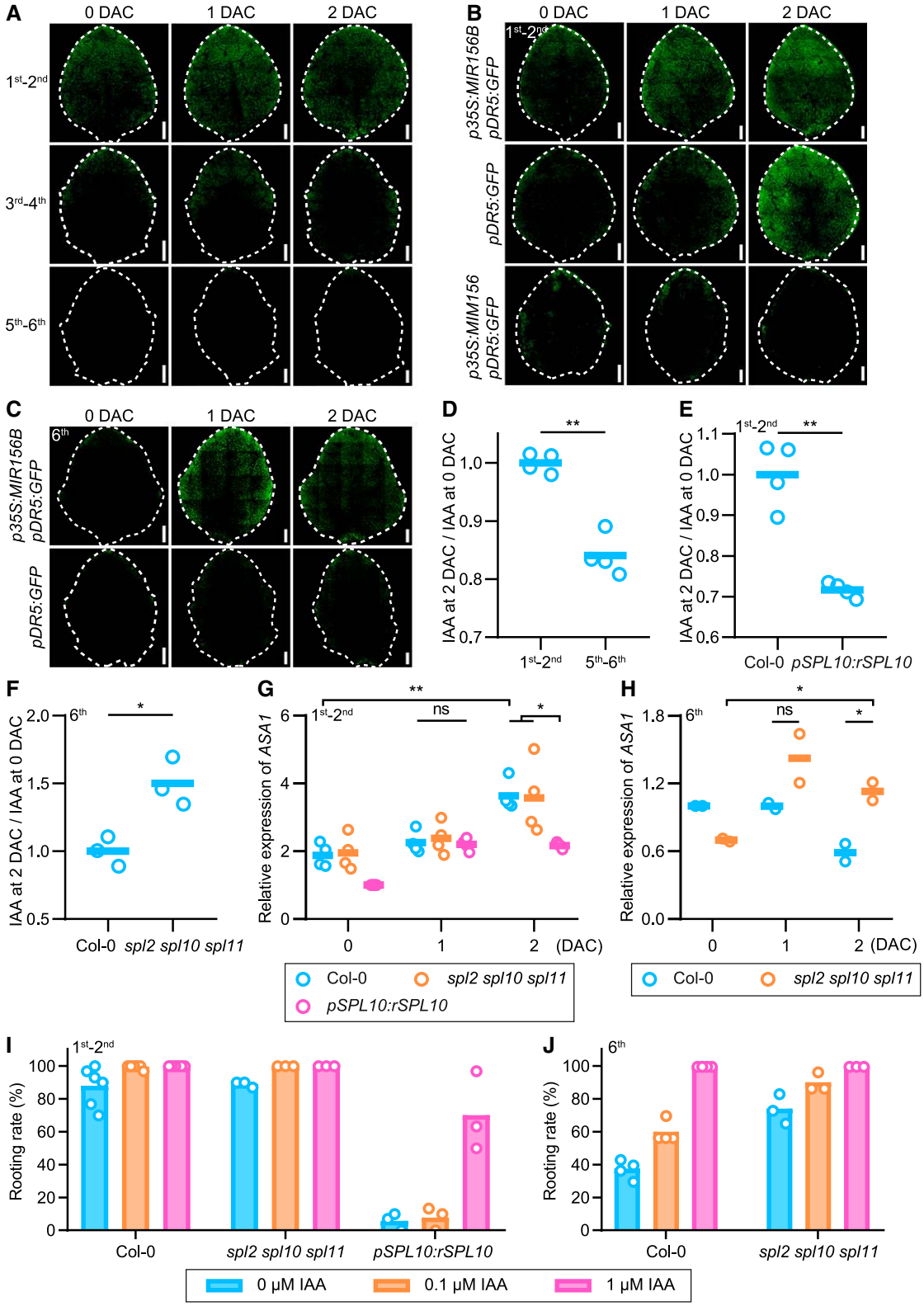

Figure 2. SPL10 Subfamily Regulates Rooting Capacity through Auxin.

expressed (twofold, $P < 0.01$). Among them, 63% of the genes (2,057/3,221) were upregulated and 37% of the genes (1,164/3,221) were downregulated (Figure 3A; Supplemental Data Sets 1 and 2). Gene ontology (GO) enrichment analysis revealed that the upregulated genes were enriched with the genes involved in jasmonic acid (JA) signaling, chitin response, and substance transportation (Supplemental Figure 6A; Supplemental Data Set 3). Further comparison with the RNA-seq data of *pSPL10:rSPL10* leaf explants identified that 590 wound-induced genes (28% [590/2,057]) were repressed by SPL10 (Figure 3A; Supplemental Data Set 4, twofold, $P < 0.01$).

The RNA-seq analyses revealed that SPL10 has a global impact on wounding response by affecting expression of >3,000 genes involved in multiple plant hormone and physiological processes. However, some of these effects may be indirect. To resolve this question, we mapped the SPL10 targets in vivo by ChIP-seq using the 3xFLAG epitope-tagged version of rSPL10 expressed under its own promoter (*pSPL10:3xFLAG-rSPL10*). *pSPL10:3xFLAG-rSPL10* showed the similar phenotype as *pSPL10:rSPL10* (Supplemental Figures 6B and 6C). The explants after 4 h of leaf detachment were harvested and subjected to ChIP-seq analysis. In total, we identified ~10,506 SPL10 binding peaks (corresponding to 8,569 genes) in the genome (Supplemental Data Set 5), in which 233 genes were wound-induced and SPL10-repressed (Figure 3C; Supplemental Data Set 6). GO analysis further revealed that the genes in response to JA, salicylic acid (SA), and wounding were overrepresented (Figures 3D to 3F; Supplemental Data Set 7). Among them, 28 genes encoded transcription factors, belonging to 12 different transcription factor families (Table 1).

De novo motif analyses revealed eight enriched putative transcription factor binding elements under SPL10 binding peaks. As expected, many peaks contain perfect GTAC motifs, the core binding motif for SPL transcription factors (Figure 3B; Klein et al., 1996). Interestingly, the binding motifs for basic helix-loop-helix, MYB, and NAC transcription factors were also enriched (Supplemental Figure 6E), implying that the transcription factors belonging to these three gene families may play a collaborative role with SPL10 in root regeneration.

Convergence of Age and Wound Signals on a Subset of *AP2/ERFs*

One of the primary events of the response to wounding that occur at the wounded site is the burst of JA (Savatin et al., 2014; Chen et al., 2016a; Hilleary and Gilroy, 2018). Our GO analyses revealed that SPL10 represses JA signaling and biosynthesis during root regeneration. Indeed, a recent article has demonstrated that miR156-targeted SPLs can stabilize JA ZIM-domain proteins, the repressor of JA signaling pathway, thereby attenuating JA responses (Mao et al., 2017).

ChIP-seq also identified eight *AP2/ERFs* as direct targets of SPL10 (Figure 4A; Supplemental Data Sets 1 and 5; Licausi et al., 2013). The binding of SPL10 on *ABSCISIC ACID REPRESSOR1* (*ABR1*) promoter was verified by ChIP-PCR analysis and competitive electrophoretic mobility shift assay (EMSA; Figure 4B; Supplemental Figures 7A to 7C). Interestingly, *ERF109* expression has been shown to be induced by JA (Cai et al., 2014). RT-qPCR analyses found that another seven *AP2/ERFs* genes also responded to JA treatment (Figures 4C to 4F; Supplemental Figures 7D to 7G). Time-course analyses further revealed that these *AP2/ERFs* were rapidly induced after leaf detachment and reduced to the basal levels after 1 to 2 h (Figure 4G; Supplemental Figures 7H and 8A). Consistent with RNA-seq data, the induction of *AP2/ERFs* was largely compromised in *pSPL10:rSPL10* leaf explants (Figure 4G; Supplemental Figures 7H and 8A). Taken together, these results suggest that age and wound signals converge on *AP2/ERF*s during root regeneration.

Figure 2. (continued).

(A) Auxin responsiveness in wild type. Auxin responsiveness is inferred by *pDR5:GFP* reporter. The leaves from the plants of different ages (first to second, third to fourth, fifth to sixth) were used as explants. Four independent experiments were performed ($n > 15$ for each experiment). One representative result is shown. The leaf shape is marked with dashed lines. Scale bar = 500 μm.

(B) and **(C)** Auxin responsiveness in wild-type, *p35S:MIR156*, and *p35S:MIM156* plants. The first to second **(B)** or sixth leaves **(C)** were used as explants. Three independent experiments were performed ($n > 15$ for each experiment). One representative result is shown. The leaf shape is marked with dash lines. Scale bars = 500 μm.

(D) Wound-induced IAA accumulation in wild-type leaf explants was attenuated in old plants. The ratio was calculated by IAA concentration at 2 DAC/IAA concentration at 0 DAC. The accumulation of auxin at the wound after leaf detachment at 2 DAC has been reported (Xu, 2018). The IAA ratio in the first to second wild-type leaf explants was set to 1. Four independent experiments were performed. Lines show mean. Two-sided Student's *t* test was performed. $^{**}P < 0.01$.

(E) and **(F)** Wound-induced IAA accumulation was modulated by SPL10 subfamily. The first to second **(E)** or sixth leaves **(F)** were used as explants. The IAA ratio in the first to second **(E)** or sixth **(F)** wild-type leaf explants was set to 1.0. Four **(E)** and three **(F)** independent experiments were performed, respectively. Lines show mean. Two-sided Student's *t* test was performed. $^{*}P < 0.05$; $^{**}P < 0.01$.

(G) and **(H)** The expression level of *ASA1* in the first to second **(G)** or six **(H)** leaf explants from wild type, *spl2 spl10 spl1*, and *pSPL10:rSPL10* at 0, 1, and 2 DAC. The expression levels in the leaves of *pSPL10:rSPL10* at 0 DAC **(G)** and the leaves of wild type at 0 DAC **(H)** were set to 1. Four **(G)** and two **(H)** independent experiments were performed, respectively. Lines show mean. One-way ANOVA followed by a Tukey's multiple comparisons test or two-sided Student's *t* test was performed. $^{*}P < 0.05$; $^{**}P < 0.01$; ns, not significant.

(I) and **(J)** Quantitative analyses of rooting rate of the first to second **(I)** or sixth **(J)** leaf explants cultured on B5 media supplemented with IAA of different concentrations. Data of *spl2 spl10 spl11* and *pSPL10:rSPL10* were from three independent experiments. Data of wild type were from six **(I)** or four **(J)** independent experiments.

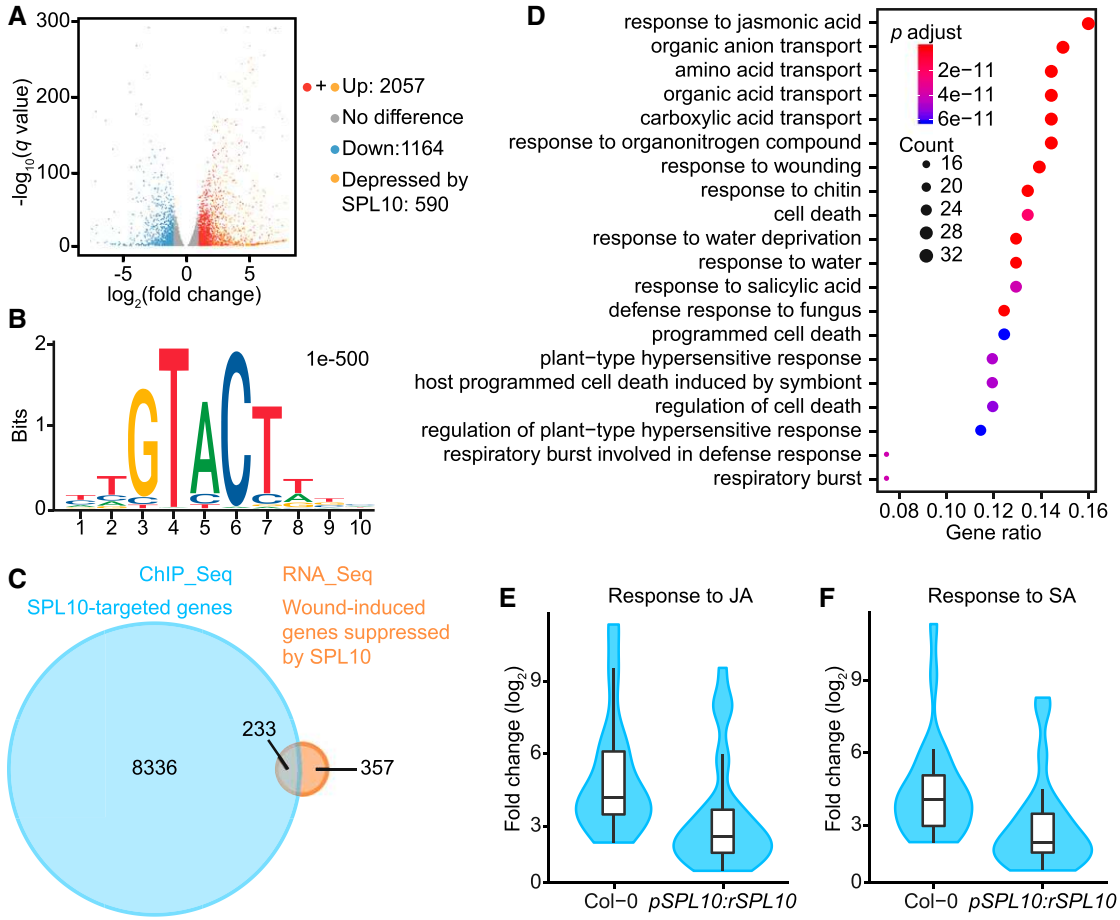

Figure 3. Identification of Downstream Targets of SPL10.

(A) Volcano plot. The explants were cultured on B5 media for 4 h and subjected to RNA-seq analyses. A total of 2,057 genes were induced, whereas 1,164 genes were repressed. *FDR* < 0.01; Log_2Fold Change > 1 or < −1. Among the wound-induced genes, 590 genes were repressed by SPL10 (1 < Log_2 FoldChange [*pSPL10:rSPL10*] < Log_2FoldChange [wild type]).
(B) The enrichment of GTAC motif in SPL10 ChIP-seq. *P* value is given at upright corner. The *e* represents times 10 raised to the power ($\times 10^n$).
(C) Venn plot. ChIP-Seq analysis revealed 8,569 genes targeted by SPL10. Among them, 233 genes were wound-inducible.
(D) GO analysis of 233 genes that are wound-induced and repressed by SPL10. The top 20 categories are shown.
(E) Fold induction of JA-responsive genes in wild type (Col-0) and *pSPL10:rSPL10* during root regeneration. The induction fold was calculated by comparison of the expression level between 0 and 4 h.
(F) Fold induction of SA-responsive genes in wild type and *pSPL10:rSPL10* during root regeneration. The induction fold was calculated by comparison of the expression level between 0 and 4 h.

The Role of *ABR1* in Root Regeneration

Previous reports have shown that ERF109 promotes lateral root initiation by activating *ASA1* gene expression (Cai et al., 2014; Kong et al., 2018), whereas ERF115 contributes to root stem cell replenishment upon damage (Heyman et al., 2013). Moreover, RELATED TO AP2 6L (RAP2.6L) is involved in tissue reunion and required for the division of pith cells in the reunion process (Asahina et al., 2011). We therefore postulate that these *AP2/ERF* genes may play important roles in wound-induced auxin biosynthesis and root regeneration. Because the enrichment of SPL10 on the *ABR1* promoter was highest among these *AP2/ERFs*, we characterized its expression and function in detail.

To reveal the expression pattern of *ABR1* during root regeneration, we generated a reporter line, in which *GUS* was expressed from the regulatory sequence of *ABR1* (*pABR1:GUS*). Under normal growth condition, GUS signals were weakly detected in leaf vascular tissues (Figure 4H). By contrast, upon wounding, the reporter expression was significantly increased at the wound after 30 min, and throughout the leaf after 1 h (Figure 4H).

To probe the role of *AP2/ERFs* in root regeneration, we generated transgenic plants that overexpressed *ABR1* using the constitutive *35S* promoter. The *p35S:ABR1* plants did not exhibit growth defects during the vegetative phase (Supplemental Figure 9A). Root regeneration assays revealed that *p35S:ABR1* conferred a higher root regenerative capacity than wild type (Figures 5A and 5B; Supplemental Figure 9C). Notably, *p35S:ABR1*

Table 1. List of 28 Genes Encoding Transcription Factors, Induced By Wounding and Suppressed by SPL10.

Gene Family	Number	Arabidopsis Genome Initiative Number and Gene Name			
B3	2	AT3G11580 (*NGAL2*)	AT5G06250 (*NGAL3*)	—	—
bHLH	3	AT1G10585	AT2G43010 (*PIF4*)	AT5G61270 (*PIF7*)	—
C2H2	1	AT2G37430 (*ZAT11*)	—	—	—
DBB	1	AT1G78600 (*BBX22*)	—	—	—
AP2/ERF	8	AT1G43160 (*RAP2.6*)	AT3G50260 (*CEJ1*)	AT4G06746 (*RAP2.9*)	AT4G34410 (*ERF109*)
		AT5G07310 (*ERF115*)	AT5G13330 (*RAP2.6L*)	AT5G53290 (*CRF3*)	AT5G64750 (*ABR1*)
LBD	1	AT2G28500 (*LBD11*)	—	—	—
MYB	2	AT2G47190 (*MYB2*)	AT4G21440 (*MYB102*)	—	—
MYB_related	1	AT3G23250 (*MYB15*)	—	—	—
NAC	2	AT1G52890 (*NAC019*)	AT3G04070 (*NAC047*)	—	—
SRS	1	AT5G12330 (*LRP1*)	—	—	—
Trihelix	2	AT2G38250	AT5G01380	—	—
WRKY	4	AT1G80840 (*WRKY40*)	AT5G07100 (*WRKY26*)	AT5G46350 (*WRKY8*)	AT5G49520 (*WRKY48*)

The gene family, the number of the genes within the same family, and accession numbers are shown. Dashes indicate no data.

was sufficient to rescue the low root regenerative capacity in *pSPL10*:*rSPL10* plants (Figures 5C and 5D; Supplemental Figure 9D), supporting the notion that *ABR1* acts downstream of SPL10/11.

AP2/ERFs constitute a large family that shares highly conserved DNA binding domains, resulting in much redundancy (Asahina et al., 2011; Licausi et al., 2013; Gu et al., 2017; Phukan et al., 2017). To overcome this, we overexpressed a dominant-negative version of ABR1 by fusion ABR1 with the repressor motif SRDX (Hiratsu et al., 2003). Compared to wild type, the rooting capacity of *p35S:ABR1-SRDX* was completely abolished (Figures 5G and 5H; Supplemental Figure 9E). To validate our results, we obtained a T-DNA insertion mutant of *abr1* and *erf109*, which did not exhibit growth defects during vegetative phase compared to wild type (Supplemental Figure 9B). Rooting assays revealed that *erf* single mutants did not exhibit strong defects in rooting, whereas *abr1 erf109* double mutant showed a lower rooting rate than wild type (Figures 5E, 5F, and 5I). The defect of *abr1 erf109* mutant was less severe than *p35S:ABR1-SRDX*, suggesting that the other six SPL10/11-regulated *AP2/ERF* genes may play redundant roles in root regeneration.

It has been shown that JA activates root stem cells (Chen et al., 2011; Marhava et al., 2019; Zhou et al., 2019). In addition, JA and ERF109 evoke auxin biosynthesis through *ASA1* (Sun et al., 2009; Cai et al., 2014). To investigate whether ABR1 also promotes root regeneration by directly binding to the *ASA1* promoter, we generated transgenic plants in which 3xFLAG-tagged *ABR1* was expressed under a constitutive *RIBO* promoter (*pRIBO:ABR1-3xFLAG*, Supplemental Figure 9F). ChIP-PCR experiments found that ABR1-3xFLAG could bind to the GCC-box in the promoter of *ASA1* (Figure 5J). Consistent with this, the induction of *ASA1* was largely compromised in *erf109 abr1* mutants (Supplemental Figure 9G), accompanied by a lower level of IAA (Figure 5K; Supplemental Figure 9H). Taken together, these results indicate that both ERF109 and ABR1 promote auxin production and rooting by activating *ASA1*.

DISCUSSION

Nature of the Wound Signal during Plant Regeneration

The very early responses to wounding include the changes in trans-membrane potential, increase of apoplastic glutamate, influx of Ca^{2+}, and generation of H_2O_2 (Lup et al., 2016; Choi et al., 2017; Toyota et al., 2018). However, how these signals regulate gene expression in the nucleus is largely unknown. The identification of wound-induced *AP2/ERFs* suggests the early wound signal rapidly reprograms the transcriptome at the transcriptional level (Marhava et al., 2019; Zhang et al., 2019; Zhou et al., 2019). Intriguingly, studies from the Sugimoto lab have shown that another group of AP2/ERF-type transcriptional factor genes, named *WOUND-INDUCED DEDIFFERENTIATION1* (*WIND1*) and its homologs *WIND2*, *WIND3* and *WIND4*, is induced upon wounding (Iwase et al., 2011a; 2011b). Importantly, transient overexpression of *WIND* genes is able to promote callus formation at the wound. These results collectively imply that *AP2/ERFs* act as a proxy for wounding signal to evoke downstream gene expression and different groups of AP2/ERFs may trigger divergent regeneration processes (Heyman et al., 2018).

How the wound signal induces *AP2/ERF* expression remains to be elucidated. Expression analyses reveal that *AP2/ERFs* such as *ABR1*, *ERF115*, and *ERF109* are induced not only by wounding but also by plant hormones such as abscisic acid, ethylene, JA, and SA, suggesting a common property shared by the *ERF* promoters. Interestingly, a recent report reveals the mechanism by which *ERF1* is rapidly induced by JA (An et al., 2017). The transcriptional coactivator complex Mediator directly links JA receptor CORONATINE INSENSITIVE1 to the *ERF1* promoter, thereby facilitating CORONATINE INSENSITIVE1-dependent degradation of JA ZIM-domain transcriptional repressors. In this scenario, we speculate that the acute induction of the wound-induced *AP2/ERFs* may be triggered by the rapid degradation of unknown transcriptional repressors that bind to the *AP2/ERF* promoters before wounding.

SPL10 Suppresses Root Regeneration through Multiple Pathways

The identification of *AP2/ERF*s as the direct of SPL10 suggests that SPL10 suppresses root regeneration by modulating auxin biosynthesis. However, we could not exclude the possibility that SPL10 regulates root regeneration via other pathways. Indeed, exogenous auxin does not fully rescue the reduced rooting

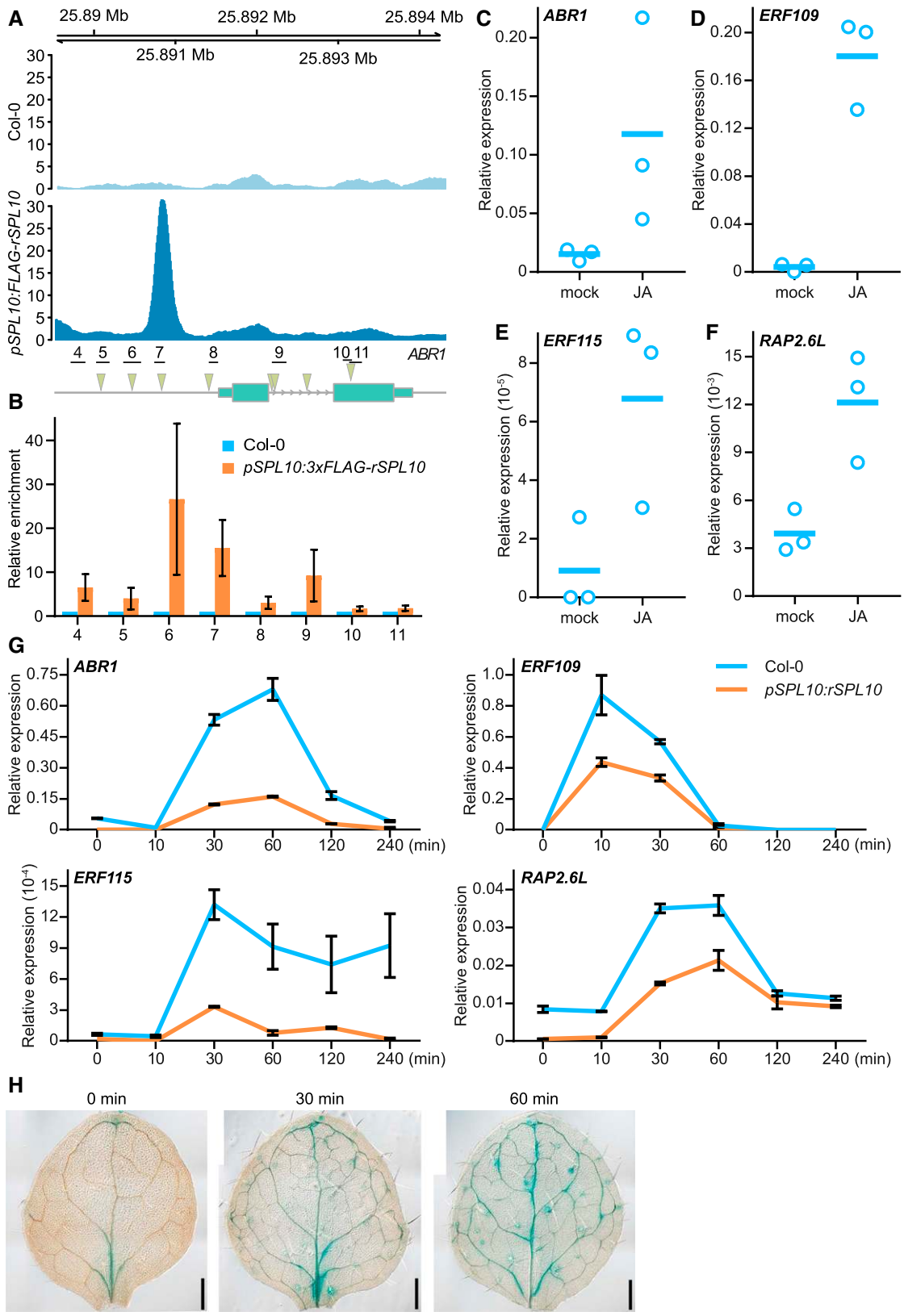

Figure 4. *AP2/ERFs* Are Direct Target of SPL10.

defects of *pSPL10*:*rSPL10*. Moreover, our GO analysis reveals that SPL10 has a broad impact on hormone responses such as ethylene, JA, and SA. Growing evidence suggests that ethylene and SA act as rooting stimuli. For example, ethylene enhances adventitious root production in petunia (*Petunia* sp) cuttings and Arabidopsis hypocotyls (Druege et al., 2014; Veloccia et al., 2016). SA triggers adventitious rooting by hydrogen peroxide in mung bean (*Vigna radiata*) seedlings (Yang et al., 2013). Therefore, it will not be surprising that SPL10 suppresses root regeneration by attenuating ethylene and SA response in the leaf explants.

The Role of SPL10 in Adventitious Root Regeneration and Lateral Root Initiation

It has been shown that SPL10 regulates lateral root number in Arabidopsis (Yu et al., 2015b; Gao et al., 2018). Plants overexpressing miR156 produce more lateral roots whereas reducing miR156 levels leads to fewer lateral roots. The identified SPL10-AP2/ERF-ASA1 cascade is unlikely to be adopted for lateral root development because the wound-inducible *AP2*/*ERFs* are not expressed under normal growth conditions. This notion is supported by findings that, although adventitious root and lateral root converge on a similar mechanism for root primordium development, their upstream events are completely different (Verstraeten et al., 2014; Birnbaum, 2016; Druege et al., 2016; Sheng et al., 2017).

miR390, TAS3-derived trans-acting short-interfering RNAs, and AUXIN RESPONSE FACTORs form an auxin-responsive regulatory network controlling lateral root growth (Marin et al., 2010; Yoon et al., 2010; He et al., 2018). Interestingly, miR390 has a similar role in vegetative phase transition as miR156 (Adenot et al., 2006; Fahlgren et al., 2006; Hunter et al., 2006). Hence, it is possible that miR156-SPL regulates lateral root initiation through miR390-ARF pathway and its precise molecular mechanism, if true, needs further investigations.

METHODS

Plant Materials and Culture Conditions

Arabidopsis (*Arabidopsis thaliana*; ecotype Columbia-0) were grown at 21°C under a 16-h light/8-h dark condition with a light intensity of 80 mmol/m^2/s using TLD 36W/865 and 36W/830 bulbs (Philips). The *p35S*:*MIR156*, *p35S*:*MIM156*, *pSPL9*:*rSPL9-GR*, *spl9 spl15*, and *pDR5*:*GFP* lines have been described in Franco-Zorrilla et al. (2007), Müller and Sheen (2008), and Wang et al. (2008, 2009). *p35S*:*MIR156 Populus x canadensis* has been described in Wang et al. (2011). The *spl2* (SALK_022235), *spl10* (Wiscseq_DsLox339A09), *erf109* (SALK_206786), and *abr1* (SALK_012151) were ordered from the Arabidopsis Biological Resource Centre. The *erf109 abr1* double mutant was identified in F2 population by PCR genotyping.

Generation of Transgenic Plants

For transgenic Arabidopsis plants, the binary constructs were delivered into *Agrobacterium tumefaciens* GV3101 (pMP90) by the freeze-thaw method. Transgenic plants were generated by the floral dipping method (Clough and Bent, 1998) and screened with 0.05% (v/v) glufosinate (Basta; BASF) on soil, 40 mg/mL of hygromycin, or 50 mg/mL of kanamycin on 1/2 Murashige and Skoog plates.

Constructs

The oligonucleotide primers for all constructs are given in Supplemental Data Set 8.

For *pSPL10*:*rSPL9*, *pSPL9*:*rSPL10*, *pSPL10*:*rSPL9-GR*, and *pSPL9*:*rSPL10-GR*, *pSPL9* and *pSPL10* fragments were PCR-amplified using *pSPL9*:*rSPL9-GR* and *pSPL10*:*rSPL10-GR* as templates. *ABR1* and *ABR1-SRDX* fragments were amplified using genomic DNA as template and then inserted into JW807. For *pSPL10*:*3xFLAG-rSPL10*, the *rSPL10* fragment was inserted into *pBSK*:*3xFLAG-X*. The *3xFLAG-rSPL10* was then digested and replaced the *rSPL10-GR* fragment in *pSPL10*:*rSPL10-GR*. For *pRIBO*:*ABR1-3xFLAG*, *ABR1* was cloned into *pBSK*:*X-3xFLAG*. The *ABR1-3xFLAG* was then digested and inserted into TQ120 behind *RIBO* promoter. *pSPL9*:*GUS*, *pSPL10*:*GUS*, and *pABR1*:*GUS* were constructed by inserting the promoters of *SPL9*, *SPL10*, and *ABR1*, respectively, into *pBB00* in the front of the *GUS* coding gene.

Root Regeneration Assay

For Arabidopsis root regeneration, seeds were germinated on half strength Murashige and Skoog medium at 21°C under a 16-h light/8-h dark condition. Leaves at same developmental stage (3 mm in length) were detached and cultured on B5 medium without Suc at 21°C under a 16-h light/8-h dark condition. The rooting rate was represented by the percentage of explants with regenerated roots in a given number of explants at 20 DAC. The regenerative capacity was represented by the percentage of leaf explants with different number of regenerated roots at 12 DAC (Chen et al., 2014). For each experiment, 30 to 40 explants were used. For DEX induction experiment, 10 μM of DEX was added into B5 medium. Water solution with an equal volume of ethanol was used as mock. For root regeneration assay in poplar tree (*Populus*), the side shoots from the wild-type and *p35S*:*MIR156* plants were detached and cultured in water. The

Figure 4. (continued).

(A) ChIP-seq data showing that SPL10 binds to the promoter region of *ABR1*. Schematic of *ABR1* gene shows the regions for ChIP-PCR analysis and the locations of SPL10 binding motif (GTAC; inverted triangles). The data was shown by Gviz (Hahne and Ivanek, 2016).
(B) ChIP-PCR analysis. Data are from three independent experiments. Bars show mean ± sd.
(C) to **(F)** Expression of *AP2*/*ERF* transcription factors in response to JA treatment. For *ABR1* and *ERF109*, explants were treated with JA for 30 min. For *ERF115* and *RAP2.6L*, the explants were treated for 60 min. Data are from three independent experiments. Lines show mean.
(G) Time course analyses of *AP2*/*ERFs* during root regeneration. Two independent experiments were performed. One representative data are shown. Bars show mean ± SD. *X*-axis stands for the culturing time after leaf detachment. Result for another biological replicate is shown in Supplemental Figure 8.
(H) GUS staining of *pABR1*:*GUS*. The leaves were detached and stained at 0, 30, and 60 min. Scale bar = 200 μm. Three independent experiments were performed (n = 15 for each experiment). One representative picture is shown.

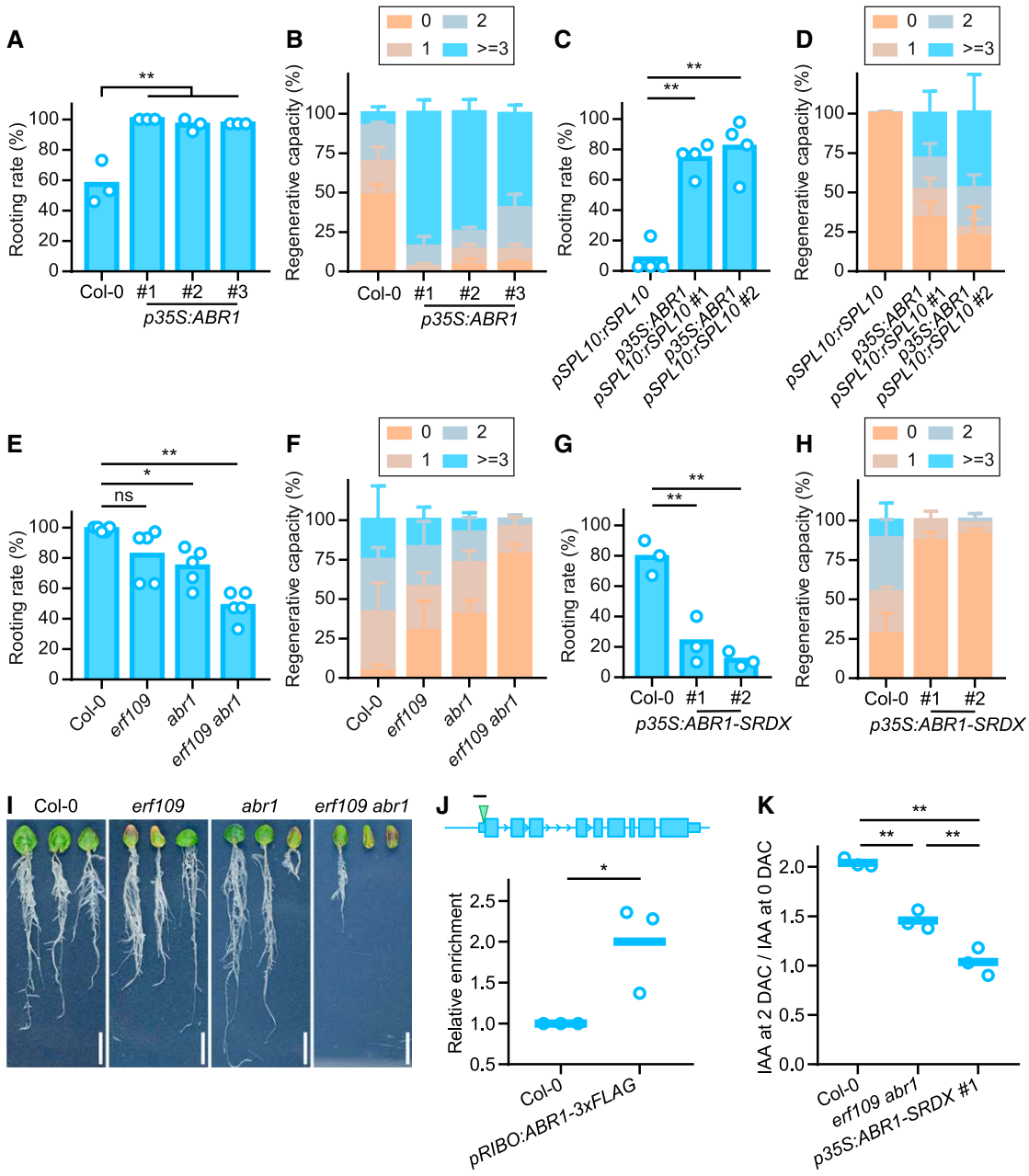

Figure 5. The Role of *ABR1* in Root Regeneration.

(A) The rooting rate of the sixth leaf explants from wild type (Col-0) and *p35S:ABR1* at 20 DAC. The rooting rate was calculated by the number of rooted explants/total number of explants. Three independent *p35S:ABR1* were used. Data are from three independent experiments. One-way ANOVA was performed followed by a Tukey's multiple comparisons test. $^{**}P < 0.001$.

(B) The regenerative capacity of the sixth leaf explants from wild type (Col-0) and *p35S:ABR1* at 12 DAC. The regenerative capacity was represented by the percentage of leaf explants with different number of regenerated roots. Three independent *p35S:ABR1* were used. Data are from three independent experiments. Bars show mean ± SD.

(C) The rooting rate of the first to second leaf explants from *pSPL10:rSPL10* and *p35S:ABR1 pSPL10:rSPL10* at 20 DAC. Data are from four independent experiments. Bars show mean. One-way ANOVA was performed followed by a Tukey's multiple comparisons test. $^{**}P < 0.01$.

(D) The regenerative capacity of the first to second leaf explants from *pSPL10:rSPL10* and *p35S:ABR1 pSPL10:rSPL10* at 12 DAC. Data are from four independent experiments. Bars show mean ± SD.

(E) The rooting rate of the first to second leaf explants from *erf* mutants at 20 DAC. Data are from five independent experiments. Bars show mean. One-way ANOVA was performed followed by a Tukey's multiple comparisons test. $^{*}P < 0.05$; $^{**}P < 0.01$; ns, not significant.

regenerative capacity was scored after 20 d. The statistical tests are shown in Supplemental Data Set 9.

Shoot Regeneration Assay

The Arabidopsis shoot regeneration assays were performed as described by Zhang et al. (2015, 2017). The shoot regenerative capacity was represented by the number of regenerated shoots per explant. The statistical tests are shown in Supplemental Data Set 9.

Expression Analyses

Total RNA was extracted with TRIzol reagent (Invitrogen). Total RNA (1 μg) was treated with *DNase* I (1 unit/mL; Fermentas) and used for cDNA synthesis with oligo (dT) primer (Fermentas). The average expression levels and SD values were calculated from $2^{-\Delta\Delta Ct}$ values. The RT-qPCR primers for *TUB* have been described in Wang et al. (2009). The oligonucleotide primers for all genes are given in Supplemental Data Set 8. The statistical tests are shown in Supplemental Data Set 9.

For hormone treatments, methyl JA (Sigma-Aldrich) was dissolved in ethanol to 50 mM and diluted d to the final concentration of 50 μM with water. Water solution with an equal volume of ethanol was used as mock (Mao et al., 2017). Twelve-d–old wild-type (Col-0) seedlings grown under long-day conditions were treated with mock or 50 μM of methyl JA. IAA was used to rescue the rooting defects in *pSPL10*:*rSPL10* plants.

Genome Editing by CRISPR/Cas9

We used egg-cell–specific promoter-controlled CRISPR/Cas9 to generate *spl10 spl11* mutant (Wang et al., 2015b). Two sgRNAs were designed and cloned into pHEE401E as described by Wang et al. (2015b). The construct was transformed into *spl10* mutant by the floral dipping method. The plants carrying the mutation in *SPL11* were identified by PCR.

RNA-Seq Analyses

For RNA-Seq analyses, RNA was extracted using TRIzol. Library construct and deep sequencing were performed using the HiSeq 4000 Platform (Illumina) following the manufacturer's instructions (BGI). Three biological replicates were performed. For RNA-seq data analysis, adapter sequences and low-quality bases were filtered from the raw data using FASTP (Chen et al., 2018). All RNA-seq data were quantified by the tool Salmon (https://combine-lab.github.io/salmon/) using The Arabidopsis Information Resource 10 transcriptome as reference (Patro et al., 2017). The raw expression data were then imported into R using the tool tximport (Soneson et al., 2015). Before differential gene expression analysis, the genes whose total counts in 12 samples were <10 were prefiltered. The differential gene expression analysis was performed with the program DESeq2 (Love et al., 2014). The GO enrichment analysis was performed by the tool clusterProfiler in biological process, molecular function, and cell component, respectively (Yu et al., 2012). The RNA-seq data (BioProject PRJCA001184) were deposited with the Beijing Institute of Genomics Data Center (http://bigd.big.ac.cn). The statistical tests are shown in Supplemental Data Set 9.

Free IAA Analyses

Free IAA content measurement in Figures 2D, 2E, and 5K and Supplemental Figure 9H was performed as described in Wang et al. (2015a), with minor modifications in ultraperformance liquid chromatography-tandem mass spectrometer conditions.

IAA content measurement in Figure 2F and Supplemental Figure 5D was performed as described by Zhang et al. (2019). Briefly, the leaf explants from each sample were ground by liquid nitrogen, dissolved by 200 μL of phosphate buffered saline for 10 min on ice, and centrifuged at 12,000 rpm at 4°C for 10 min. The auxin concentration was measured with 10 μL of supernatant for each technical repeat using electrochemical detection of auxin as described by Sun et al. (2017, 2018). The statistical tests are shown in Supplemental Data Set 9.

ChIP-PCR and ChIP-seq Analyses

Briefly, the first to second leaf explants from wild type (Col-0), *pSPL10*:*3xFLAG-rSPL10*, and *pRIBO*:*ABR1-3xFLAG* were cultured on B5 medium, harvested after 4 h, and fixed according to a published protocol (Yu et al., 2013). The chromatin extract was immunoprecipitated with anti-FLAG beads (cat. nos. SA042001 and SA042005; Sigma-Aldrich). ChIP DNAs were reverse cross linked and purified with a PCR purification kit (cat. no. 28,206; Qiagen). One microliter of DNA was used for RT-qPCR analyses. The relative enrichment of 3×FLAG-rSPL10 and ABR1-3×FLAG was calculated by normalizing the amount of each immunoprecipitated fragment to input DNA, and then by normalizing the value for transgenic plants against the value for wild-type as a negative control.

For ChIP-seq data analysis, all ChIP-seq reads were first aligned to the Arabidopsis genome (The Arabidopsis Information Resource 10) with the software BowTie2 (Langmead and Salzberg, 2012). After marking duplicated reads with the program sambamba (Tarasov et al., 2015), we used the SAMtools program (Li et al., 2009) to filter duplicates (only DNA sequencing), unmapped reads, ambiguously mapped reads, and read pairs with conflicting alignments. To assess the correlation between replicates, we computed the reads coverage for consecutive bins of 10 kilobases with deepTools (Ramírez et al., 2014). Pearson correlation was then used for the

Figure 5. (continued).

(F) The regenerative capacity of the first to second leaf explants from *erf* mutants at 12 DAC. Data are from five independent experiments. Bars show mean ± SD.

(G) The rooting rate of the first to second leaf explants from wild type (Col-0) and *p35S*:*ABR1-SRDX* at 20 DAC. Data are from three independent experiments. Bars show mean. One-way ANOVA was performed followed by a Tukey's multiple comparisons test. $^{**}P < 0.01$.

(H) The regenerative capacity of the first to second leaf explants from wild type (Col-0) and *p35S*:*ABR1-SRDX* at 12 DAC. Data are from three independent experiments. Bars show mean ± sd.

(I) Root regeneration assays using wild type and *erf* mutants. Pictures were taken at 20 DAC. Scale bar = 1 cm.

(J) ChIP-PCR analysis showing enrichment of *ABR1-3xFLAG* on the promoter of *ASA1*. Schematic of *ASA1* genomic region shows the region for ChIP-PCR analysis (black overbar) and the location of GCC-box (inverted green triangles). The enrichment level in wild type (Col-0) was set to 1. Data are from three independent experiments. Bars show mean. Two-sided Student's *t* test was performed. $^{*}P < 0.05$.

(K) Wound-induced IAA accumulation in the first to second leaf explants from wild type and *ERF* mutant. The IAA ratio in the first to second leaf explants of *p35S*:*ABR1-SRDX* #1 was set to 1. Three independent experiments were performed. Lines show mean. One-way ANOVA was performed followed by a Tukey's multiple comparisons test. $^{**}P < 0.01$.

analysis. All the ChIP-seq peaks were called by MACS2 with default parameters (Zhang et al., 2008). BEDTools (Quinlan and Hall, 2010) was used to identify the specific peak in *pSPL10*:*3xFLAG-rSPL10*. To find the sequence motif enriched in ChIP-seq peaks, findMotifsGenome.pl from the HOMER program was used (Heinz et al., 2010). The tool ChIPseeker was then used to retrieve the nearest genes around the peak (Yu et al., 2015a). Two biological replicates were performed. The statistical tests are shown in Supplemental Data Set 9.

GUS Staining

For *pSPL9*:*GUS*, *pSPL10*:*GUS*, and *pABR1*:*GUS* staining, explants were incubated in a GUS assay solution (100 mM of sodium phosphate buffer, 10 mM of EDTA, 0.1% [v/v] Triton X-100, and 0.1% [w/v] X-Gluc) at 37°C. The chlorophyll of the stained tissues were removed by incubating with 75% alcohol at room temperature for 12 h, and then in chloral hydrate solution (200 g of chloral hydrate, 20 g of glycerol, and 50 mL of water at 65°C for ~12 h, until tissues became transparent (Tsuge et al., 1996). The Differential Interference Contrast observations were conducted using a BX63 microscope (Olympus).

EMSA

To construct plasmid for expression of the DNA binding domain of SPL10 in *Escherichia coli*, the coding sequence of *SPL10* was PCR-amplified and cloned into pRSF-Duet (https://www.helmholtz-muenchen.de/fileadmin/PEPF/pRSF_vectors/pRSFDuet-1_map.pdf). Oligonucleotide probes were synthesized and labeled with biotin at the 5′ end. EMSA was performed using a LightShift Chemiluminescent EMSA Kit (catalog no. 20148X; Thermo Fisher Scientific). Briefly, biotin-labeled probes were incubated in 1× binding buffer, 5 mM of $MgCl_2$, 0.05% (v/v) NP-40, and 50 ng/μL of Poly (dI·dC) with or without proteins at room temperature for 20 min. For unlabeled probe competition, unlabeled probes were added to the reactions.

Microscopy

For confocal imaging, we used a model no. LSM880 confocal microscopic system (Zeiss) to observe GFP fluorescence.

Accession Numbers

Sequence data from this article can be found in the Arabidopsis Genome Initiative or GenBank/European Molecular Biology Laboratory databases under the following accession numbers: SPL2 (At5g43270), SPL9 (At2g42200), SPL10 (At1g27370), SPL11 (At1g27360), SPL15 (At3g57920), TUB (At5g62690), ABR1 (At5g64750), ERF109 (At4g34410), ERF115 (AT5g07310), RAP2.6L (At5g13330), RAP2.6 (At1g43160), RAP2.9 (At4g06746), CEJ1 (At3g50260), CRF3 (At5g53290), ASA1 (At5g05730), and TAA1 (At1g70560). The ChIP-seq data (BioProject PRJCA001184) were deposited with the Beijing Institute of Genomics Data Center (http://bigd.big.ac.cn).

Supplemental Data

Supplemental Figure 1. Developmental decline of rooting capacity.

Supplemental Figure 2. Generation of *spl10 spl11* double mutant and phenotypic analyses.

Supplemental Figure 3. Plant phenotype and expression pattern of *SPL* GUS reporters.

Supplemental Figure 4. Rooting phenotype.

Supplemental Figure 5. Age and SPL10 subfamily regulate rooting capacity through auxin.

Supplemental Figure 6. RNA-seq and ChIP-seq analyses.

Supplemental Figure 7. *AP2/ERF* genes are the direct targets of SPL10.

Supplemental Figure 8. Time course analyses of *AP2/ERFs* during root regeneration.

Supplemental Figure 9. ABR1 regulates rooting capacity.

Supplemental Data Set 1. The genes upregulated after leaf detachment in wild-type leaf explants.

Supplemental Data Set 2. The genes downregulated after leaf detachment in wild-type leaf explants.

Supplemental Data Set 3. GO enrichment analysis of upregulated genes in wild-type leaf explants.

Supplemental Data Set 4. The wound-induced genes repressed by SPL10.

Supplemental Data Set 5. SPL10 binding peaks identified by ChIP-seq.

Supplemental Data Set 6. Two-hundred and thirty-three wound-induced and SPL10-repressed genes.

Supplemental Data Set 7. GO enrichment analysis of 233 candidate genes.

Supplemental Data Set 8. Oligonucleotide primer sequences.

Supplemental Data Set 9. Summary of statistical tests.

ACKNOWLEDGMENTS

We thank the Arabidopsis Biological Resource Center for seeds and Qi-Jun Chen (China Agricultural University, China) for the CRISPR/Cas9 vector; Xiao-Su Gao, Jiqin Li, Yun-Xiao He, and Shui-Ning Yang (Chinese Academy of Sciences Center for Excellence in Molecular Plant Sciences, China) for skillful technical assistance; Hongtao Liu, Lin Xu (Chinese Academy of Sciences Center for Excellence in Molecular Plant Sciences, China), and members of the J.-W. Wang lab for discussion and comments on the article; and Jijun Yan and Jinfang Chu (National Centre for Plant Gene Research, Institute of Genetics and Developmental Biology, Chinese Academy of Sciences, China) and Guochen Qin and Wenting Liu (Shanghai Center for Plant Stress Biology, Chinese Academy of Sciences Center for Excellence in Molecular Plant Sciences, China) for measuring free IAA contents. This work was supported National Key Research and Development Program (2016YFA0500800), the National Natural Science Foundation of China (grants 31430013, 31222029, 912173023, 31525004, and 31770399), and the Strategic Priority Research Program of the Chinese Academy of Sciences (grant XDB27030101).

AUTHOR CONTRIBUTIONS

B.-B.Y. and J.-W.W. designed the research; B.-B.Y. performed most of the experiments; G.-D.S. and Z.-G.X. analyzed the ChIP-seq and RNA-seq data; Y.P., N.B., L.S., and T.X. contributed to the auxin measurement; C.-M.Z. prepared the protein for EMSA experiment; Y.-B.M. analyzed JA-related data; B.-B.Y. and J.-W.W. analyzed the rest of the data; J.-W.W. wrote the article.

Received September 9, 2019; revised October 7, 2019; accepted October 24, 2019; published October 24, 2019.

REFERENCES

Adenot, X., Elmayan, T., Lauressergues, D., Boutet, S., Bouché, N., Gasciolli, V., and Vaucheret, H. (2006). DRB4-dependent TAS3 trans-acting siRNAs control leaf morphology through AGO7. Curr. Biol. **16:** 927–932.

An, C., Li, L., Zhai, Q., You, Y., Deng, L., Wu, F., Chen, R., Jiang, H., Wang, H., Chen, Q., and Li, C. (2017). Mediator subunit MED25 links the jasmonate receptor to transcriptionally active chromatin. Proc. Natl. Acad. Sci. USA **114:** E8930–E8939.

Asahina, M., et al. (2011). Spatially selective hormonal control of RAP2.6L and ANAC071 transcription factors involved in tissue reunion in Arabidopsis. Proc. Natl. Acad. Sci. USA **108:** 16128–16132.

Atta, R., Laurens, L., Boucheron-Dubuisson, E., Guivarc'h, A., Carnero, E., Giraudat-Pautot, V., Rech, P., and Chriqui, D. (2009). Pluripotency of Arabidopsis xylem pericycle underlies shoot regeneration from root and hypocotyl explants grown in vitro. Plant J. **57:** 626–644.

Aung, B., Gao, R., Gruber, M.Y., Yuan, Z.C., Sumarah, M., and Hannoufa, A. (2017). MsmiR156 affects global gene expression and promotes root regenerative capacity and nitrogen fixation activity in alfalfa. Transgenic Res. **26:** 541–557.

Berdowski, J.J.M., and Siepel, H. (1998). Vegetative regeneration of *Calluna vulgaris* at different ages and fertilizer levels. Biol. Conserv. **46:** 85–93.

Birnbaum, K.D. (2016). How many ways are there to make a root? Curr. Opin. Plant Biol. **34:** 61–67.

Birnbaum, K.D., and Sánchez Alvarado, A. (2008). Slicing across kingdoms: Regeneration in plants and animals. Cell **132:** 697–710.

Cai, X.T., Xu, P., Zhao, P.X., Liu, R., Yu, L.H., and Xiang, C.B. (2014). Arabidopsis ERF109 mediates cross-talk between jasmonic acid and auxin biosynthesis during lateral root formation. Nat. Commun. **5:** 5833.

Chen, L., Sun, B., Xu, L., and Liu, W. (2016a). Wound signaling: The missing link in plant regeneration. Plant Signal. Behav. **11:** e1238548.

Chen, L., Tong, J., Xiao, L., Ruan, Y., Liu, J., Zeng, M., Huang, H., Wang, J.W., and Xu, L. (2016b). YUCCA-mediated auxin biogenesis is required for cell fate transition occurring during de novo root organogenesis in Arabidopsis. J. Exp. Bot. **67:** 4273–4284.

Chen, Q., et al. (2011). The basic helix–loop–helix transcription factor MYC2 directly represses PLETHORA expression during jasmonate-mediated modulation of the root stem cell niche in Arabidopsis. Plant Cell **23:** 3335–3352.

Chen, S., Zhou, Y., Chen, Y., and Gu, J. (2018). fastp: An ultra-fast all-in-one FASTQ preprocessor. Bioinformatics **34:** i884–i890.

Chen, X., Qu, Y., Sheng, L., Liu, J., Huang, H., and Xu, L. (2014). A simple method suitable to study de novo root organogenesis. Front. Plant Sci. **5:** 208.

Choi, W.G., Miller, G., Wallace, I., Harper, J., Mittler, R., and Gilroy, S. (2017). Orchestrating rapid long-distance signaling in plants with Ca^{2+}, ROS and electrical signals. Plant J. **90:** 698–707.

Clough, S.J., and Bent, A.F. (1998). Floral dip: A simplified method for Agrobacterium-mediated transformation of *Arabidopsis thaliana*. Plant J. **16:** 735–743.

Druege, U., Franken, P., and Hajirezaei, M.R. (2016). Plant hormone homeostasis, signaling, and function during adventitious root formation in cuttings. Front. Plant Sci. **7:** 381.

Druege, U., Franken, P., Lischewski, S., Ahkami, A.H., Zerche, S., Hause, B., and Hajirezaei, M.R. (2014). Transcriptomic analysis reveals ethylene as stimulator and auxin as regulator of adventitious root formation in petunia cuttings. Front. Plant Sci. **5:** 494.

Efroni, I., Mello, A., Nawy, T., Ip, P.L., Rahni, R., DelRose, N., Powers, A., Satija, R., and Birnbaum, K.D. (2016). Root regeneration triggers an embryo-like sequence guided by hormonal interactions. Cell **165:** 1721–1733.

Fahlgren, N., Montgomery, T.A., Howell, M.D., Allen, E., Dvorak, S.K., Alexander, A.L., and Carrington, J.C. (2006). Regulation of AUXIN RESPONSE FACTOR3 by TAS3 ta-siRNA affects developmental timing and patterning in Arabidopsis. Curr. Biol. **16:** 939–944.

Franco-Zorrilla, J.M., Valli, A., Todesco, M., Mateos, I., Puga, M.I., Rubio-Somoza, I., Leyva, A., Weigel, D., García, J.A., and Paz-Ares, J. (2007). Target mimicry provides a new mechanism for regulation of microRNA activity. Nat. Genet. **39:** 1033–1037.

Gandikota, M., Birkenbihl, R.P., Höhmann, S., Cardon, G.H., Saedler, H., and Huijser, P. (2007). The miRNA156/157 recognition element in the 3′ UTR of the Arabidopsis SBP box gene SPL3 prevents early flowering by translational inhibition in seedlings. Plant J. **49:** 683–693.

Gao, R., Wang, Y., Gruber, M.Y., and Hannoufa, A. (2018). miR156/SPL10 modulates lateral root development, branching and leaf morphology in Arabidopsis by silencing *AGAMOUS-LIKE 79*. Front. Plant Sci. **8:** 2226.

Gu, C., Guo, Z.H., Hao, P.P., Wang, G.M., Jin, Z.M., and Zhang, S.L. (2017). Multiple regulatory roles of AP2/ERF transcription factor in angiosperm. Bot. Stud. (Taipei, Taiwan) **58:** 6.

Hahne, F., and Ivanek, R. (2016). Visualizing Genomic Data Using Gviz and Bioconductor. In Mathé E, Davis S (eds.), Statistical Genomics: Methods and Protocols.. (New York, USA: Springer New York).

He, F., Xu, C., Fu, X., Shen, Y., Guo, L., Leng, M., and Luo, K. (2018). The *MicroRNA390/TRANS-ACTING SHORT INTERFERING RNA3* module mediates lateral root growth under salt stress via the auxin pathway. Plant Physiol. **177:** 775–791.

Heinz, S., Benner, C., Spann, N., Bertolino, E., Lin, Y.C., Laslo, P., Cheng, J.X., Murre, C., Singh, H., and Glass, C.K. (2010). Simple combinations of lineage-determining transcription factors prime cis-regulatory elements required for macrophage and B cell identities. Mol. Cell **38:** 576–589.

Heyman, J., Cools, T., Vandenbussche, F., Heyndrickx, K.S., Van Leene, J., Vercauteren, I., Vanderauwera, S., Vandepoele, K., De Jaeger, G., Van Der Straeten, D., and De Veylder, L. (2013). ERF115 controls root quiescent center cell division and stem cell replenishment. Science **342:** 860–863.

Heyman, J., Canher, B., Bisht, A., Christiaens, F., and De Veylder, L. (2018). Emerging role of the plant ERF transcription factors in coordinating wound defense responses and repair. J. Cell. Sci. **131:** jcs208215.

Hilleary, R., and Gilroy, S. (2018). Systemic signaling in response to wounding and pathogens. Curr. Opin. Plant Biol. **43:** 57–62.

Hiratsu, K., Matsui, K., Koyama, T., and Ohme-Takagi, M. (2003). Dominant repression of target genes by chimeric repressors that include the EAR motif, a repression domain, in Arabidopsis. Plant J. **34:** 733–739.

Hunter, C., Willmann, M.R., Wu, G., Yoshikawa, M., de la Luz Gutiérrez-Nava, M., and Poethig, S.R. (2006). Trans-acting siRNA-mediated repression of ETTIN and ARF4 regulates heteroblasty in Arabidopsis. Development **133:** 2973–2981.

Ikeuchi, M., Ogawa, Y., Iwase, A., and Sugimoto, K. (2016). Plant regeneration: Cellular origins and molecular mechanisms. Development **143:** 1442–1451.

Iwase, A., Ohme-Takagi, M., and Sugimoto, K. (2011a). WIND1: A key molecular switch for plant cell dedifferentiation. Plant Signal. Behav. **6:** 1943–1945.

Iwase, A., Mitsuda, N., Koyama, T., Hiratsu, K., Kojima, M., Arai, T., Inoue, Y., Seki, M., Sakakibara, H., Sugimoto, K., and Ohme-Takagi, M. (2011b). The AP2/ERF transcription factor WIND1 controls cell dedifferentiation in Arabidopsis. Curr. Biol. **21:** 508–514.

Kareem, A., Radhakrishnan, D., Sondhi, Y., Aiyaz, M., Roy, M.V., Sugimoto, K., and Prasad, K. (2016). De novo assembly of plant body plan: A step ahead of Deadpool. Regeneration (Oxf.) **3:** 182–197.

Kartsonas, E., and Papafotiou, M. (2007). Mother plant age and seasonal influence on in vitro propagation of *Quercus euboica* Pap, an endemic, rare and endangered oak species of Greece. Plant Cell Tissue Organ Cult. **90:** 111–116.

Klein, J., Saedler, H., and Huijser, P. (1996). A new family of DNA binding proteins includes putative transcriptional regulators of the *Antirrhinum majus* floral meristem identity gene SQUAMOSA. Mol. Gen. Genet. **250:** 7–16.

Kong, X., et al. (2018). PHB3 maintains root stem cell niche identity through ROS-responsive AP2/ERF transcription factors in Arabidopsis. Cell Reports **22:** 1350–1363.

Langmead, B., and Salzberg, S.L. (2012). Fast gapped-read alignment with BowTie 2. Nat. Methods **9:** 357–359.

Li, H., Handsaker, B., Wysoker, A., Fennell, T., Ruan, J., Homer, N., Marth, G., Abecasis, G., and Durbin, R.; 1000 Genome Project Data Processing Subgroup. (2009). The Sequence Alignment/Map format and SAMtools. Bioinformatics **25:** 2078–2079.

Licausi, F., Ohme-Takagi, M., and Perata, P. (2013). APETALA2/Ethylene Responsive Factor (AP2/ERF) transcription factors: Mediators of stress responses and developmental programs. New Phytol. **199:** 639–649.

Liu, J., Sheng, L., Xu, Y., Li, J., Yang, Z., Huang, H., and Xu, L. (2014). WOX11 and 12 are involved in the first-step cell fate transition during de novo root organogenesis in Arabidopsis. Plant Cell **26:** 1081–1093.

Love, M.I., Huber, W., and Anders, S. (2014). Moderated estimation of fold change and dispersion for RNA-seq data with DESeq2. Genome Biol. **15:** 550.

Lup, S.D., Tian, X., Xu, J., and Pérez-Pérez, J.M. (2016). Wound signaling of regenerative cell reprogramming. Plant Sci. **250:** 178–187.

Mao, Y.B., Liu, Y.Q., Chen, D.Y., Chen, F.Y., Fang, X., Hong, G.J., Wang, L.J., Wang, J.W., and Chen, X.Y. (2017). Jasmonate response decay and defense metabolite accumulation contributes to age-regulated dynamics of plant insect resistance. Nat. Commun. **8:** 13925.

Marhava, P., Hoermayer, L., Yoshida, S., Marhavy, P., Benkova, E., and and Friml, J. (2019). Re-activation of stem cell pathways for pattern restoration in plant wound healing. Cell **177:** 957–969 e913.

Marin, E., Jouannet, V., Herz, A., Lokerse, A.S., Weijers, D., Vaucheret, H., Nussaume, L., Crespi, M.D., and Maizel, A. (2010). miR390, Arabidopsis TAS3 tasiRNAs, and their AUXIN RESPONSE FACTOR targets define an autoregulatory network quantitatively regulating lateral root growth. Plant Cell **22:** 1104–1117.

Müller, B., and Sheen, J. (2008). Cytokinin and auxin interaction in root stem-cell specification during early embryogenesis. Nature **453:** 1094–1097.

Patro, R., Duggal, G., Love, M.I., Irizarry, R.A., and Kingsford, C. (2017). Salmon provides fast and bias-aware quantification of transcript expression. Nat. Methods **14:** 417–419.

Perianez-Rodriguez, J., Manzano, C., and Moreno-Risueno, M.A. (2014). Post-embryonic organogenesis and plant regeneration from tissues: Two sides of the same coin? Front. Plant Sci. **5:** 219.

Phukan, U.J., Jeena, G.S., Tripathi, V., and Shukla, R.K. (2017). Regulation of Apetala2/Ethylene response factors in plants. Front. Plant Sci. **8:** 150.

Poethig, R.S. (2009). Small RNAs and developmental timing in plants. Curr. Opin. Genet. Dev. **19:** 374–378.

Porrello, E.R., Mahmoud, A.I., Simpson, E., Hill, J.A., Richardson, J.A., Olson, E.N., and Sadek, H.A. (2011). Transient regenerative potential of the neonatal mouse heart. Science **331:** 1078–1080.

Pulianmackal, A.J., Kareem, A.V., Durgaprasad, K., Trivedi, Z.B., and Prasad, K. (2014). Competence and regulatory interactions during regeneration in plants. Front. Plant Sci. **5:** 142.

Quinlan, A.R., and Hall, I.M. (2010). BEDTools: A flexible suite of utilities for comparing genomic features. Bioinformatics **26:** 841–842.

Ramírez, F., Dündar, F., Diehl, S., Grüning, B.A., and Manke, T. (2014). deepTools: A flexible platform for exploring deep-sequencing data. Nucleic Acids Res. **42:** W187–W191.

Ran, Y., Liang, Z., and Gao, C. (2017). Current and future editing reagent delivery systems for plant genome editing. Sci. China Life Sci. **60:** 490–505.

Rhoades, M.W., Reinhart, B.J., Lim, L.P., Burge, C.B., Bartel, B., and Bartel, D.P. (2002). Prediction of plant microRNA targets. Cell **110:** 513–520.

Ruckh, J.M., Zhao, J.W., Shadrach, J.L., van Wijngaarden, P., Rao, T.N., Wagers, A.J., and Franklin, R.J. (2012). Rejuvenation of regeneration in the aging central nervous system. Cell Stem Cell **10:** 96–103.

Sabatini, S., Beis, D., Wolkenfelt, H., Murfett, J., Guilfoyle, T., Malamy, J., Benfey, P., Leyser, O., Bechtold, N., Weisbeek, P., and Scheres, B. (1999). An auxin-dependent distal organizer of pattern and polarity in the Arabidopsis root. Cell **99:** 463–472.

Sang, Y.L., Cheng, Z.J., and Zhang, X.S. (2018). iPSCs: A comparison between animals and plants. Trends Plant Sci. **23:** 660–666.

Savatin, D.V., Gramegna, G., Modesti, V., and Cervone, F. (2014). Wounding in the plant tissue: The defense of a dangerous passage. Front. Plant Sci. **5:** 470.

Schwab, R., Palatnik, J.F., Riester, M., Schommer, C., Schmid, M., and Weigel, D. (2005). Specific effects of microRNAs on the plant transcriptome. Dev. Cell **8:** 517–527.

Sena, G., and Birnbaum, K.D. (2010). Built to rebuild: In search of organizing principles in plant regeneration. Curr. Opin. Genet. Dev. **20:** 460–465.

Sheng, L., Hu, X., Du, Y., Zhang, G., Huang, H., Scheres, B., and Xu, L. (2017). Non-canonical *WOX11*-mediated root branching contributes to plasticity in *Arabidopsis* root system architecture. Development **144:** 3126–3133.

Skoog, F., and Miller, C.O. (1957). Chemical regulation of growth and organ formation in plant tissues cultured in vitro. Symp. Soc. Exp. Biol. **11:** 118–130.

Soneson, C., Love, M.I., and Robinson, M.D. (2015). Differential analyses for RNA-seq: Transcript-level estimates improve gene-level inferences. F1000 Res. **4:** 1521.

Stepanova, A.N., Hoyt, J.M., Hamilton, A.A., and Alonso, J.M. (2005). A link between ethylene and auxin uncovered by the characterization of two root-specific ethylene-insensitive mutants in Arabidopsis. Plant Cell **17:** 2230–2242.

Stepanova, A.N., Robertson-Hoyt, J., Yun, J., Benavente, L.M., Xie, D.Y., Dolezal, K., Schlereth, A., Jürgens, G., and Alonso, J.M. (2008). TAA1-mediated auxin biosynthesis is essential for hormone crosstalk and plant development. Cell **133:** 177–191.

Su, Y.H., and Zhang, X.S. (2014). The hormonal control of regeneration in plants. Curr. Top. Dev. Biol. **108:** 35–69.

Sugimoto, K., Jiao, Y., and Meyerowitz, E.M. (2010). Arabidopsis regeneration from multiple tissues occurs via a root development pathway. Dev. Cell **18:** 463–471.

Sun, J., et al. (2009). Arabidopsis ASA1 is important for jasmonate-mediated regulation of auxin biosynthesis and transport during lateral root formation. Plant Cell **21:** 1495–1511.

Sun, L., Xie, Y., Yan, Y., Yang, H., Gu, H., and Bao, N. (2017). Paper-based analytical devices for direct electrochemical detection of free IAA and SA in plant samples with the weight of several milligrams. Sens. Actuators B Chem. **247:** 336–342.

Sun, L., Zhou, J., Pan, J., Liang, Y., Fang, Z., Xie, Y., Yang, H., Gu, H., and Bao, N. (2018). Electrochemical mapping of indole-3-acetic acid and salicylic acid in whole pea seedlings under normal conditions and salinity. Sens. Actuators B Chem. **276:** 545–551.

Tao, Y., et al. (2008). Rapid synthesis of auxin via a new tryptophan-dependent pathway is required for shade avoidance in plants. Cell **133:** 164–176.

Tarasov, A., Vilella, A.J., Cuppen, E., Nijman, I.J., and Prins, P. (2015). Sambamba: Fast processing of NGS alignment formats. Bioinformatics **31:** 2032–2034.

Toyota, M., Spencer, D., Sawai-Toyota, S., Jiaqi, W., Zhang, T., Koo, A.J., Howe, G.A., and Gilroy, S. (2018). Glutamate triggers long-distance, calcium-based plant defense signaling. Science **361:** 1112–1115.

Tsuge, T., Tsukaya, H., and Uchimiya, H. (1996). Two independent and polarized processes of cell elongation regulate leaf blade expansion in *Arabidopsis thaliana* (L.) Heynh. Development **122:** 1589–1600.

Veloccia, A., Fattorini, L., Della Rovere, F., Sofo, A., D'Angeli, S., Betti, C., Falasca, G., and Altamura, M.M. (2016). Ethylene and auxin interaction in the control of adventitious rooting in *Arabidopsis thaliana*. J. Exp. Bot. **67:** 6445–6458.

Verstraeten, I., Schotte, S., and Geelen, D. (2014). Hypocotyl adventitious root organogenesis differs from lateral root development. Front. Plant Sci. **5:** 495.

Wang, B., Chu, J., Yu, T., Xu, Q., Sun, X., Yuan, J., Xiong, G., Wang, G., Wang, Y., and Li, J. (2015a). Tryptophan-independent auxin biosynthesis contributes to early embryogenesis in Arabidopsis. Proc. Natl. Acad. Sci. USA **112:** 4821–4826.

Wang, J.W., Czech, B., and Weigel, D. (2009). miR156-regulated SPL transcription factors define an endogenous flowering pathway in *Arabidopsis thaliana*. Cell **138:** 738–749.

Wang, J.W., Schwab, R., Czech, B., Mica, E., and Weigel, D. (2008). Dual effects of miR156-targeted SPL genes and CYP78A5/KLUH on plastochron length and organ size in *Arabidopsis thaliana*. Plant Cell **20:** 1231–1243.

Wang, J.W., Park, M.Y., Wang, L.J., Koo, Y., Chen, X.Y., Weigel, D., and Poethig, R.S. (2011). miRNA control of vegetative phase change in trees. PLoS Genet. **7:** e1002012.

Wang, Z.P., Xing, H.L., Dong, L., Zhang, H.Y., Han, C.Y., Wang, X.C., and Chen, Q.J. (2015b). Egg cell-specific promoter-controlled CRISPR/Cas9 efficiently generates homozygous mutants for multiple target genes in Arabidopsis in a single generation. Genome Biol. **16:** 144.

Wells, J.M., and Watt, F.M. (2018). Diverse mechanisms for endogenous regeneration and repair in mammalian organs. Nature **557:** 322–328.

Wu, G., and Poethig, R.S. (2006). Temporal regulation of shoot development in *Arabidopsis thaliana* by miR156 and its target SPL3. Development **133:** 3539–3547.

Xing, S., Salinas, M., Garcia-Molina, A., Höhmann, S., Berndtgen, R., and Huijser, P. (2013). SPL8 and miR156-targeted SPL genes redundantly regulate *Arabidopsis gynoecium* differential patterning. Plant J. **75:** 566–577.

Xu, L. (2018). De novo root regeneration from leaf explants: Wounding, auxin, and cell fate transition. Curr. Opin. Plant Biol. **41:** 39–45.

Xu, L., and Huang, H. (2014). Genetic and epigenetic controls of plant regeneration. Curr. Top. Dev. Biol. **108:** 1–33.

Xu, L., Hu, Y., Cao, Y., Li, J., Ma, L., Li, Y., and Qi, Y. (2018). An expression atlas of miRNAs in *Arabidopsis thaliana*. Sci. China Life Sci. **61:** 178–189.

Xu, M., Hu, T., Zhao, J., Park, M.Y., Earley, K.W., Wu, G., Yang, L., and Poethig, R.S. (2016). Developmental functions of miR156-regulated SQUAMOSA PROMOTER BINDING PROTEIN-LIKE (SPL) genes in *Arabidopsis thaliana*. PLoS Genet. **12:** e1006263.

Xu, X., Li, X., Hu, X., Wu, T., Wang, Y., Xu, X., Zhang, X., and Han, Z. (2017). High miR156 expression is required for auxin-induced adventitious root formation via *MxSPL26* independent of *PINs* and *ARFs* in *Malus xiaojinensis*. Front. Plant Sci. **8:** 1059.

Yamaguchi, A., Wu, M.F., Yang, L., Wu, G., Poethig, R.S., and Wagner, D. (2009). The microRNA-regulated SBP-Box transcription factor SPL3 is a direct upstream activator of LEAFY, FRUITFULL, and APETALA1. Dev. Cell **17:** 268–278.

Yang, W., Zhu, C., Ma, X., Li, G., Gan, L., Ng, D., and Xia, K. (2013). Hydrogen peroxide is a second messenger in the salicylic acid-triggered adventitious rooting process in mung bean seedlings. PLoS One **8:** e84580.

Ye, B.B., Zhang, K., and Wang, J.W. (2019). The role of miR156 in rejuvenation in *Arabidopsis thaliana*. J. Integr. Plant Biol..

Yin, K., Gao, C., and Qiu, J.L. (2017). Progress and prospects in plant genome editing. Nat. Plants **3:** 17107.

Yoon, E.K., Yang, J.H., Lim, J., Kim, S.H., Kim, S.K., and Lee, W.S. (2010). Auxin regulation of the microRNA390-dependent transacting small interfering RNA pathway in Arabidopsis lateral root development. Nucleic Acids Res. **38:** 1382–1391.

Yu, G., Wang, L.G., and He, Q.Y. (2015a). ChIPseeker: An R/Bioconductor package for ChIP peak annotation, comparison and visualization. Bioinformatics **31:** 2382–2383.

Yu, G., Wang, L.G., Han, Y., and He, Q.Y. (2012). clusterProfiler: An R package for comparing biological themes among gene clusters. OMICS **16:** 284–287.

Yu, N., Niu, Q.W., Ng, K.H., and Chua, N.H. (2015b). The role of miR156/SPLs modules in Arabidopsis lateral root development. Plant J. **83:** 673–685.

Yu, S., Lian, H., and Wang, J.W. (2015c). Plant developmental transitions: The role of microRNAs and sugars. Curr. Opin. Plant Biol. **27:** 1–7.

Yu, S., Cao, L., Zhou, C.M., Zhang, T.Q., Lian, H., Sun, Y., Wu, J., Huang, J., Wang, G., and Wang, J.W. (2013). Sugar is an endogenous cue for juvenile-to-adult phase transition in plants. eLife **2:** e00269.

Zhang, G., Zhao, F., Chen, L., Pan, Y., Sun, L., Bao, N., Zhang, T., Cui, C.X., Qiu, Z., Zhang, Y., Yang, L., and Xu, L. (2019). Jasmonate-mediated wound signalling promotes plant regeneration. Nat. Plants **5:** 491–497.

Zhang, T.Q., Lian, H., Zhou, C.M., Xu, L., Jiao, Y., and Wang, J.W. (2017). A two-step model for de novo activation of *WUSCHEL* during plant shoot regeneration. Plant Cell **29:** 1073–1087.

Zhang, T.Q., Lian, H., Tang, H., Dolezal, K., Zhou, C.M., Yu, S., Chen, J.H., Chen, Q., Liu, H., Ljung, K., and Wang, J.W. (2015). An intrinsic microRNA timer regulates progressive decline in shoot regenerative capacity in plants. Plant Cell **27:** 349–360.

Zhang, Y., Liu, T., Meyer, C.A., Eeckhoute, J., Johnson, D.S., Bernstein, B.E., Nusbaum, C., Myers, R.M., Brown, M., Li, W., and Liu, X.S. (2008). Model-based analysis of ChIP-seq (MACS). Genome Biol. **9:** R137.

Zhou, W., Lozano-Torres, J.L., Blilou, I., Zhang, X., Zhai, Q., Smant, G., Li, C., and and Scheres, B. (2019). A jasmonate signaling network activates root stem cells and promotes regeneration. Cell **177:** 942–956 e914.